Nanoparticle Accumulation and Transcytosis in Brain Endothelial Cell Layers

Dong Ye,[a] Michelle Nic Raghnaill,[a] Mattia Bramini,[a] Eugene Mahon,[a] Christoffer Åberg,[a] Anna Salvati,*[a] Kenneth A. Dawson*[a]

[a] Centre for BioNano Interactions, School of Chemistry and Chemical Biology & UCD Conway Institute for Biomolecular and Biomedical Research, University College Dublin, Belfield, Dublin 4, Ireland.

Supplementary Information

Table S1. Hydrodynamic diameter of SiO_2 nanoparticles (100 μg/ml) in water and 2 % FBS assay medium. The average hydrodynamic diameter of commercially available 50 nm, 100 nm, and 200 nm SiO_2-NPs in water showed sizes close to the nominal (labeled) size, with low polydispersity index (PDI) values. The average diameter and PDI of the SiO_2-NP dispersions increased in cell culture medium, indicating partial agglomeration when proteins are added. Errors are the standard deviation of 3 replicates (11 runs each). For a more complete characterization of the same particles see Shapero et al., Molecular BioSystems, 2011, 7, 371-378.

SiO_2 NPs nominal size	Temperature (^oC)	Hydrodynamic diameter in de-ionized water (nm)[a]	PDI in water[b]	Hydrodynamic diameter in 2% FBS assay medium (nm)[a]	PDI in 2% FBS assay medium[b]
50 nm	37	52 ± 2	0.17	134 ± 3	0.37
100 nm	37	101 ± 6	0.02	170 ± 12	0.34
200 nm	37	193 ± 11	0.04	217 ± 13	0.19

[a] z-average hydrodynamic diameter extracted by cumulant analysis of the data. [b] Polydispersity index from cumulant fitting.

Table S2. Hydrodynamic diameter of gold nanoparticles in 2 % FBS assay medium. Au nanoparticles of 5, 12 and 25 nm were conjugated with transferrin (Tf) and human serum albumin (HSA). Additional particles conjugated with polyethylene glycol of different molecular weight were also prepared (PEG, 5k and 20k). The characterisation of the conjugated nanoparticles in cell culture medium indicated relatively good nanoparticle dispersions with partial agglomeration observed in some cases.

Gold NPs	T (^{o}C)	Hydrodynamic diameter (± SD) in 2% FBS assay medium (nm)[a]	PDI in 2% FBS assay medium[b]
Au 5nm -Tf	37	29 ± 1	0.52
Au 5nm -HSA	37	37 ± 1	0.35
Au 12nm-HSA	37	27 ± 1	0.18
Au 12nm-Tf	37	76 ± 19	0.21
Au 25nm-Tf	37	101 ± 2	0.23
Au 12nm-PEG 5k	37	33 ± 4	0.22
Au 12nm-PEG 20k	37	50 ± 5	0.19

[a] z-average hydrodynamic diameter extracted by cumulant analysis of the data. [b] Polydispersity index from cumulant fitting.

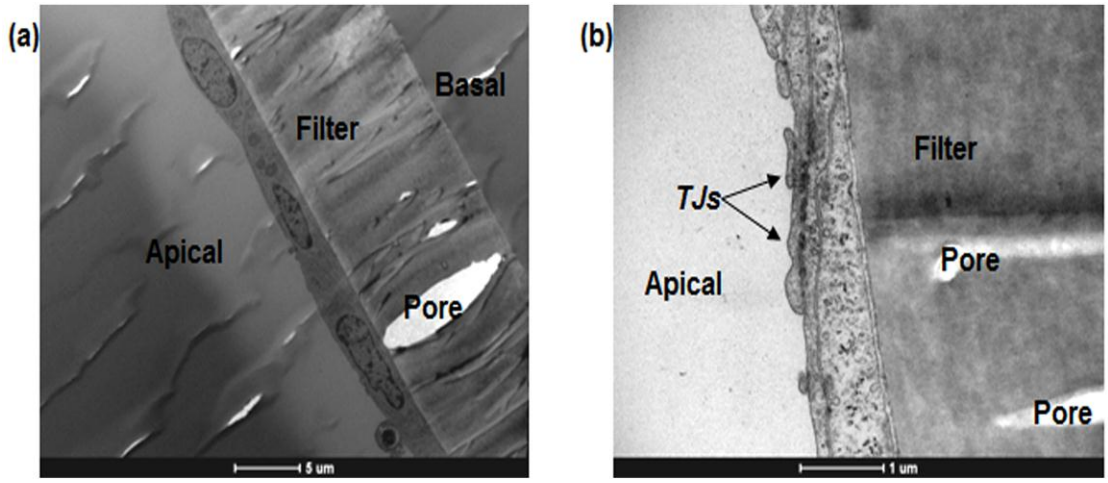

Figure S1. Formation of a cell monolayer and tight junction expression in the BBB transwell system. Human brain capillary microvascular endothelial cells (hCMEC/D3) were cultured in growth-factor depleted EGM-2 medium for 7 days on type I collagen coated, 0.4 μm polyester transwell filters. A cross section of the endothelial cell barrier was cut out along with the polyester filter membrane and analyzed on a TECNAI 12 transmission electron microscope at 120 kV. (a) TEM imaging shows that a homogenous cell monolayer as thin as approximately 1-2 μm could be obtained. The barrier cells exhibited a spindle-shaped and elongated phenotype. (b) Formation of tight junctions (TJs) among membranes of adjacent cells was also observed, as indicated by arrows.

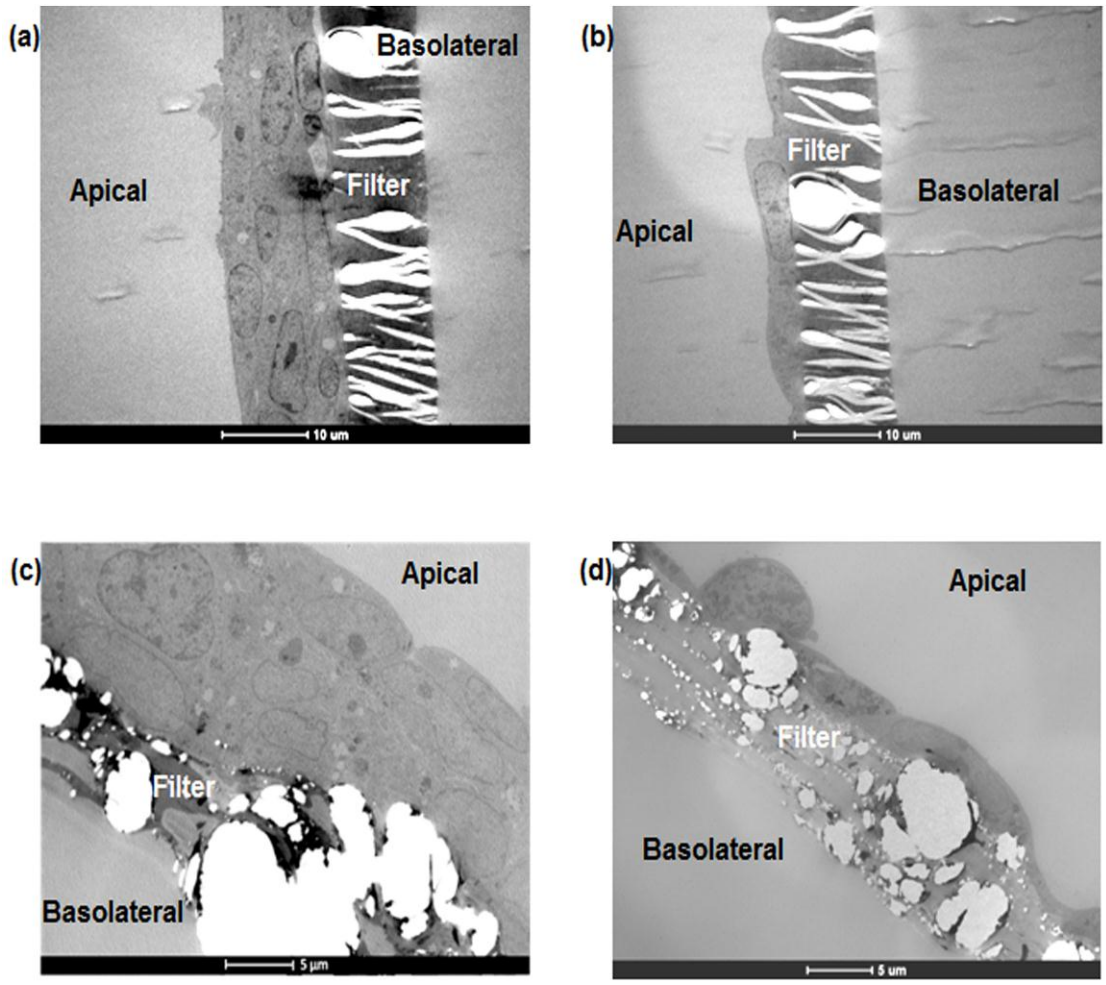

Figure S2. Presence of areas of cell multilayers in some BBB transwell systems. On polycarbonate transwells of pore size 0.4 µm, hCMEC/D3 endothelial cells formed, in some areas, both (a) multilayers, and (b) monolayers. Similarly, on 3.0 µm PTFE transwells, the presence of both (c) multilayers and (d) monolayers was observed. Optimised cell culture techniques, as described in the Methods and main text, were therefore applied for cell growth, in order to ensure the formation of an extended well-differentiated monolayer.

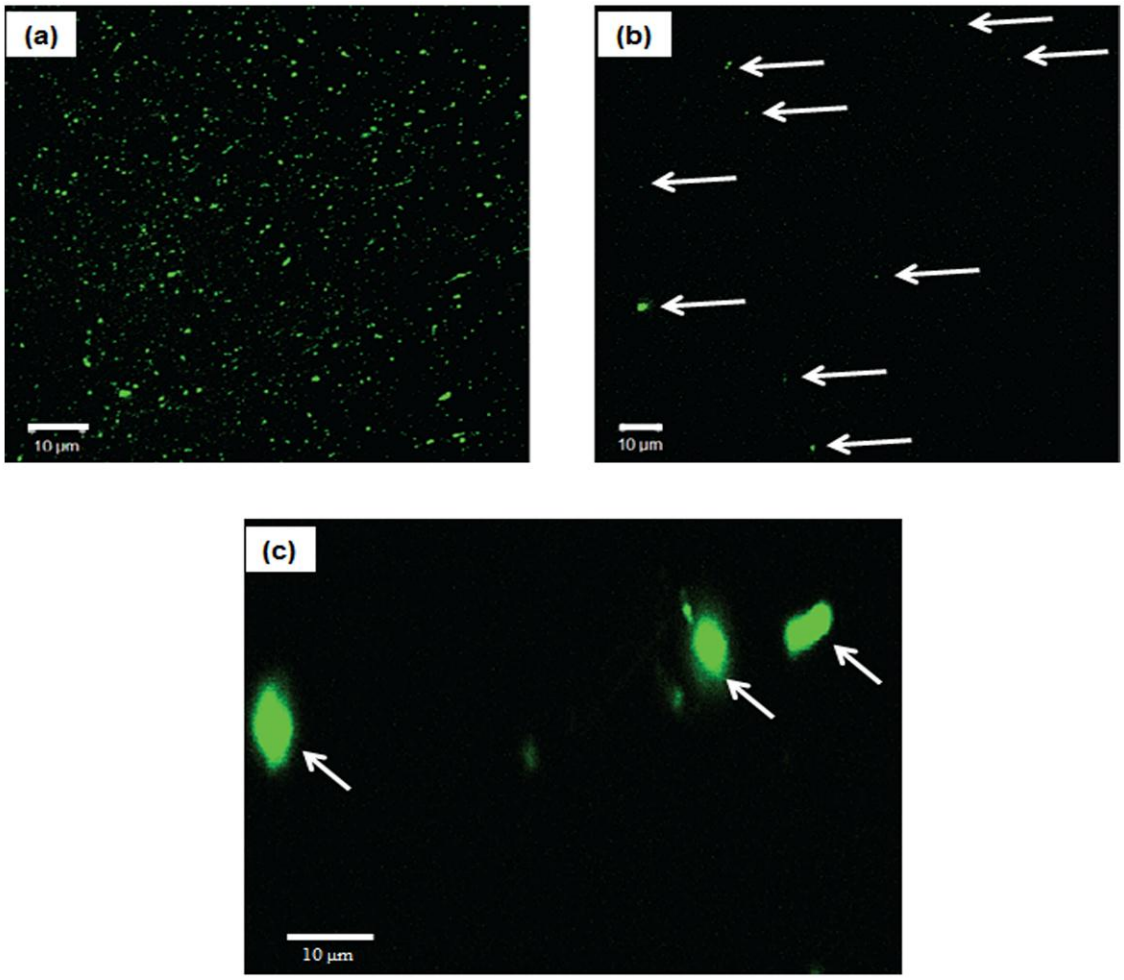

Figure S3. Fluorescence imaging of nanoparticles in the apical and basal chambers of transwell systems. Fluorescence microscopy imaging was performed on the solutions taken from the apical and basolateral chambers of a 3.0 µm porous transwell following 4-hour exposure of the BBB monolayer to 100 µg/ml 50 nm SiO_2 nanoparticles. (a) In the medium recovered from the apical chamber, nanoparticles were clearly detected. (b) In the basolateral medium, even though fluorescence intensity measurements indicated, in some cases, very high signals in comparisons to the intensity of the apical nanoparticle dispersion (data not shown), only few nanoparticles were observed by fluorescence microscopy. This confirms that at most few nanoparticles may have translocated across the BBB. However, simple fluorescence measurements may be affected by the eventual presence in the nanoparticles of a fraction of labile dye which could leak to the basolateral chamber. (c) The medium recovered from the basal chamber also showed the presence of large fluorescent aggregates (white arrows) whose fluorescence signal was approximately 5 µm in diameter. These may be due to particle agglomerates or some debris.

These large debris of fluorescent material in the basolateral chamber can scatter light, thus causing incorrect fluorescence intensity measurements.

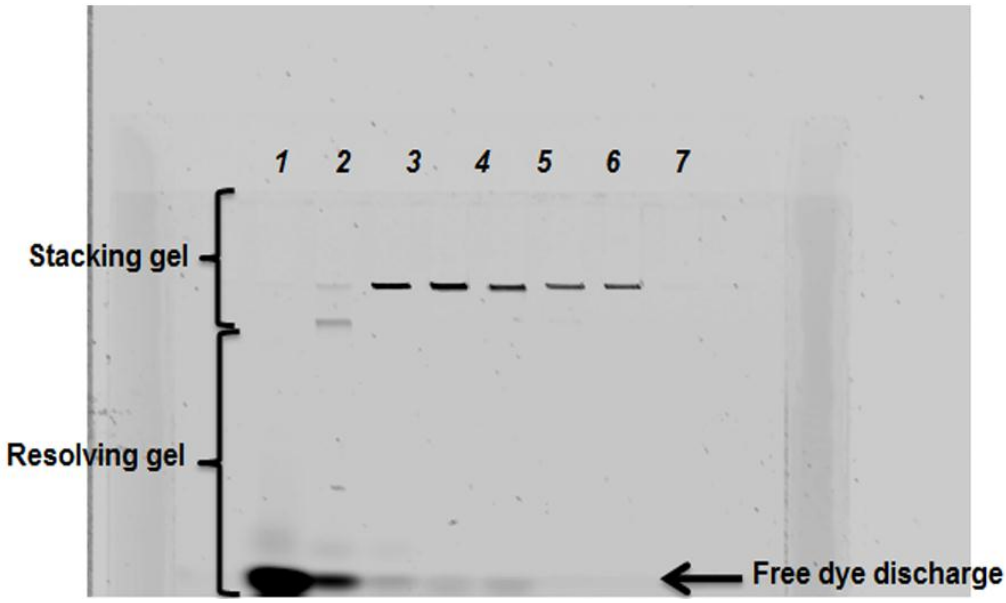

Figure S4. Fluorescence image of an SDS-PAGE of the nanoparticles used for the study. Samples are, in order from lane 1 to 7: 4 kDa FITC-dextran, examples of 30 nm, 50 nm and 150 nm SiO_2-NPs (synthesized in house), and finally the 50 nm, 100 nm and 200 nm SiO_2-NPs used for the study (from Kisker Scientific). All nanoparticles were suspended in water. The gel can be used to detect the presence of labile free dye in the nanoparticle dispersions. While nanoparticles are usually too small to enter the gel (with the exception of the smaller 30 nm silica in lane 2 which enter to a limited extent), labile free dye can be separated and detected at the bottom of the gel. The gel shows that a small amount of free dye could be detected in the 50 nm SiO_2-NPs used for the study (lane 5).

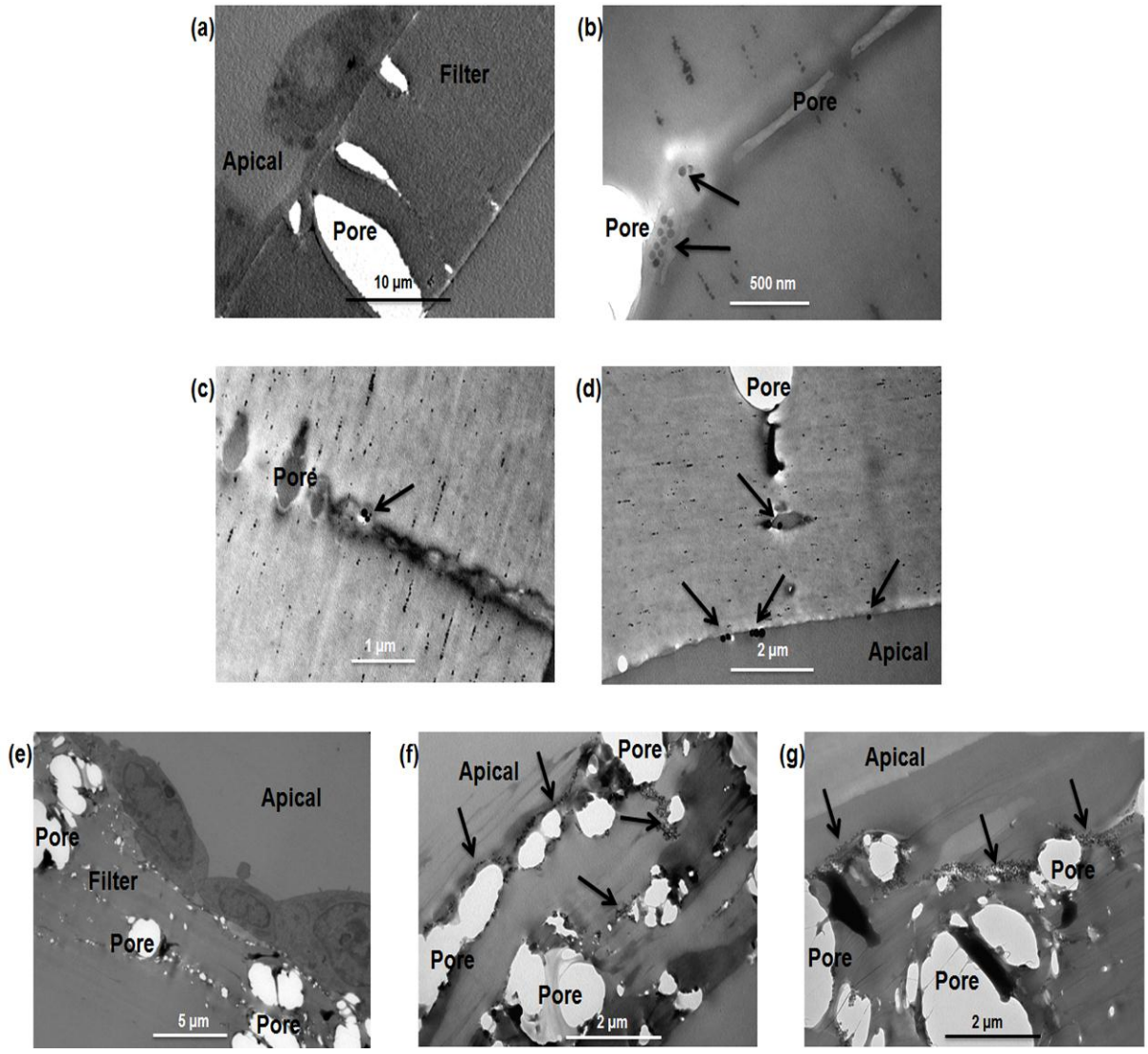

Figure S5. Adhesion of silica nanoparticles to the pores of some transwell systems. In order to test if the nanoparticles used for the study could adhere to the filter, thus affecting the nanoparticle transport studies, different types of transwell filters (empty wells without cells) were exposed to silica nanoparticles (100 µg/ml) at 37°C for 4 hours (panels b-d and f-g). Then, particle dispersions were removed from the apical and basolateral chambers. Transwells with cells grown on top but not exposed to nanoparticles are also shown as controls (panels a and e). The transwells were embedded with epoxy resin and cross sections of the filters were sliced with a microtome as described in the Methods to allow TEM imaging. TEM results showed that (b) 50 nm, (c) 100 nm and (d) 200 nm SiO_2-NPs all remained in the pores of 0.4 µm polyester (PET) transwells. No sign of nanoparticle-like structures were found (a) when the same transwells were

not exposed to nanoparticles, suggesting that the nanoparticles indicated in panels b-c are, indeed, nanoparticles, and not structures originating from the porous membrane itself. 50 nm SiO_2-NPs were also tested in (f) 0.4 μm and (g) 3.0 μm porous polytetrafluoroethylene (PTFE) membranes. Again, no signs of nanoparticle-like structures (e) could be found for the 3.0 μm PTFE membranes not exposed to nanoparticles. Comparatively larger amounts of 50 nm silica nanoparticles were found adhering to the pore walls of PTFE membranes. (Note also that all filters were burnt after exposure to the electron beam. Therefore, the sizes of the pores shown in the images may be significantly changed compared to their original sizes.)

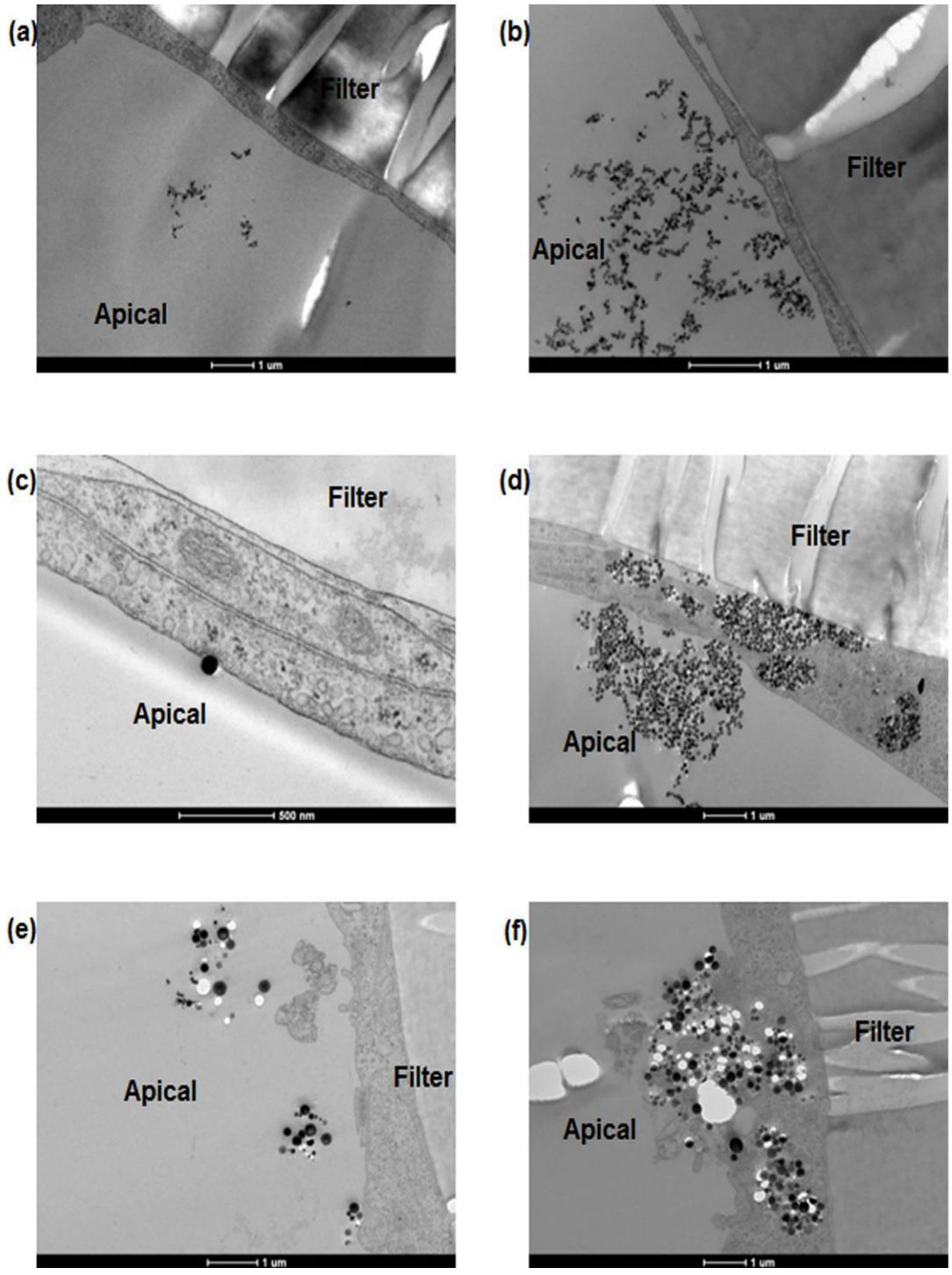

Figure S6. Overview of the BBB monolayer exposed to silica nanoparticles. TEM imaging showed that in different sections of the same samples, very different amounts of nanoparticles interacting with the cell membrane could be observed. For instance, for the 50 nm silica nanoparticles, in some cases, (a) very few SiO_2 nanoparticles were observed close to the cell monolayer, while in other sections, (b) large clusters of nanoparticles were found close to the cell

membrane. Similarly, for cells exposed to 100 nm SiO_2 nanoparticles, both (c) single nanoparticles and (d) large clusters were observed, both outside and inside the cells, close to the bottom of the monolayer. (e-f) Similar images were found also for cells exposed to 200 nm SiO_2 nanoparticles.

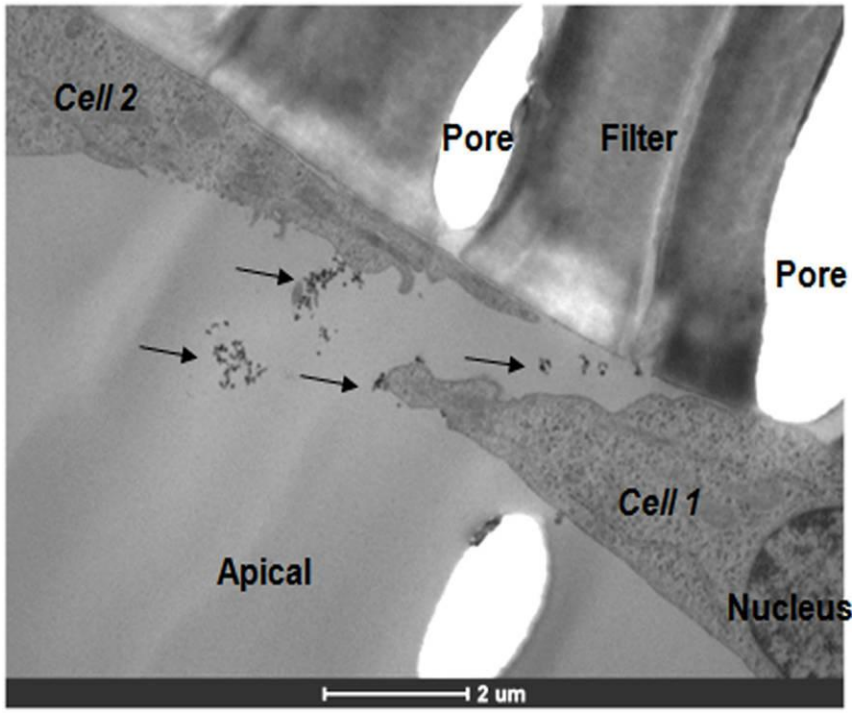

Figure S7. Indications of monolayer interruptions and imperfections. In some cases, TEM imaging indicated that the BBB monolayer did not fully cover the whole surface of the transwell filter: in this image, a small interruption to the barrier integrity could be observed between two neighbouring cells (Cell 1 and 2). This could potentially allow nanoparticles to reach the filter membrane and pass to the basolateral chamber, potentially even being internalised by the cell from the basolateral side. This could then be misinterpreted as transcytosis. The arrows indicate some 50 nm SiO_2 nanoparticles approaching the filter in the area where cells are not in contact.

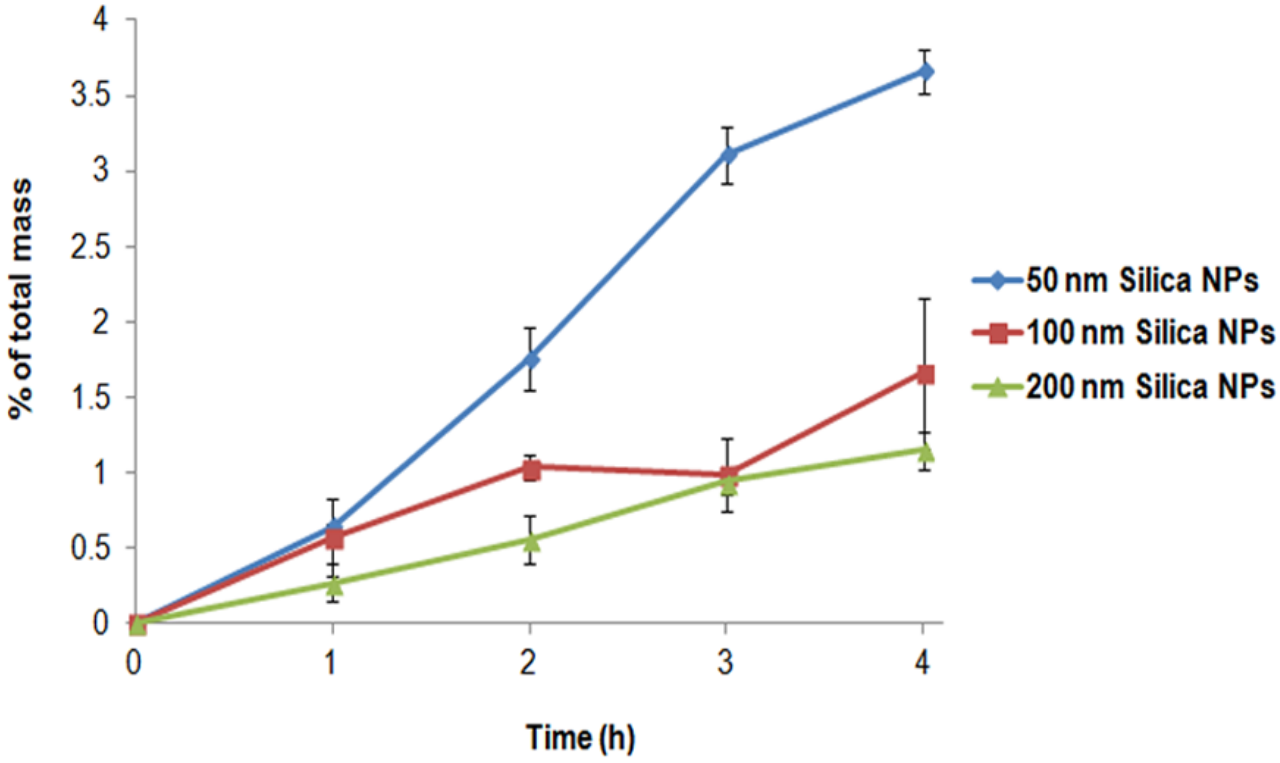

Figure S8. Transport of silica nanoparticles across the hCMEC/D3 BBB model in a transwell setup. Green fluorescent silica nanoparticles of different sizes (50, 100 and 200 nm; 100 µg/ml) were exposed to cells at 37 ^{o}C for 4 hours (see Methods for details) and the transport into the basal chamber was calculated by quantifying the fluorescence intensity of the medium in the basolateral chamber as described in the Methods. The results showed that the mass of silica nanoparticles in the basolateral chamber was 3.6 %, 1.7 %, and 1.1 % of the total mass applied for the 50, 100 and 200 nm silica nanoparticles, respectively. This suggests that transcytosis is low for these particles (at least on this time scale). However, as discussed in the text, these studies can be significantly affected by particle loss inside the filter pores, as well as the eventual presence of a fraction of labile dye released from the nanoparticles and defects in the cell monolayer.

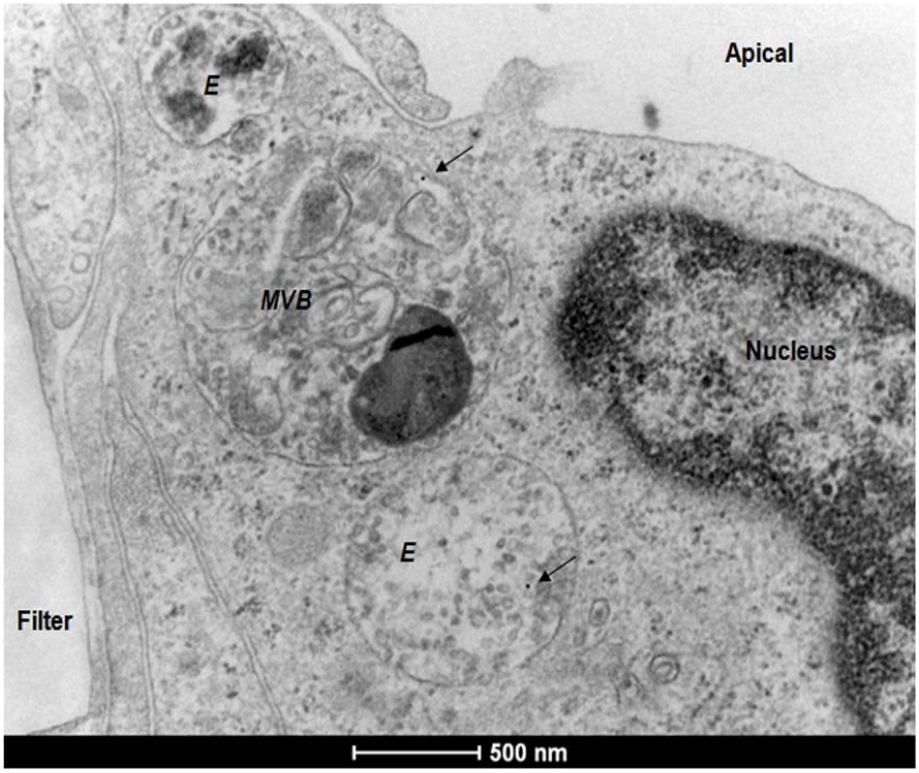

Figure S9. Uptake and transcytosis of 12 nm PEGylated Au-NPs in hCMEC/D3 cell monolayers. Cells were exposed to 50 µg/ml nanoparticles in 2% FBS assay medium for 4 hours. TEM imaging showed that overall the uptake of these nanoparticles was relatively low. After 4 hours of exposure, Au-NPs were found in multivesiclular bodies (*MVB*), endosomes (*E*), and other vesicles along the endo-lysosomal pathway. The arrows indicate some of the internalised nanoparticles. It should be noted that such nanoparticles can be easily distinguished from cellular structures due to their higher electron density; in cases of doubt, further magnification was performed under which gold nanoparticles remain sharp and clear while cellular structures become blurry. Similar intracellular locations were found also for the other PEGylated Au particles tested (5 and 25 nm; data not shown).

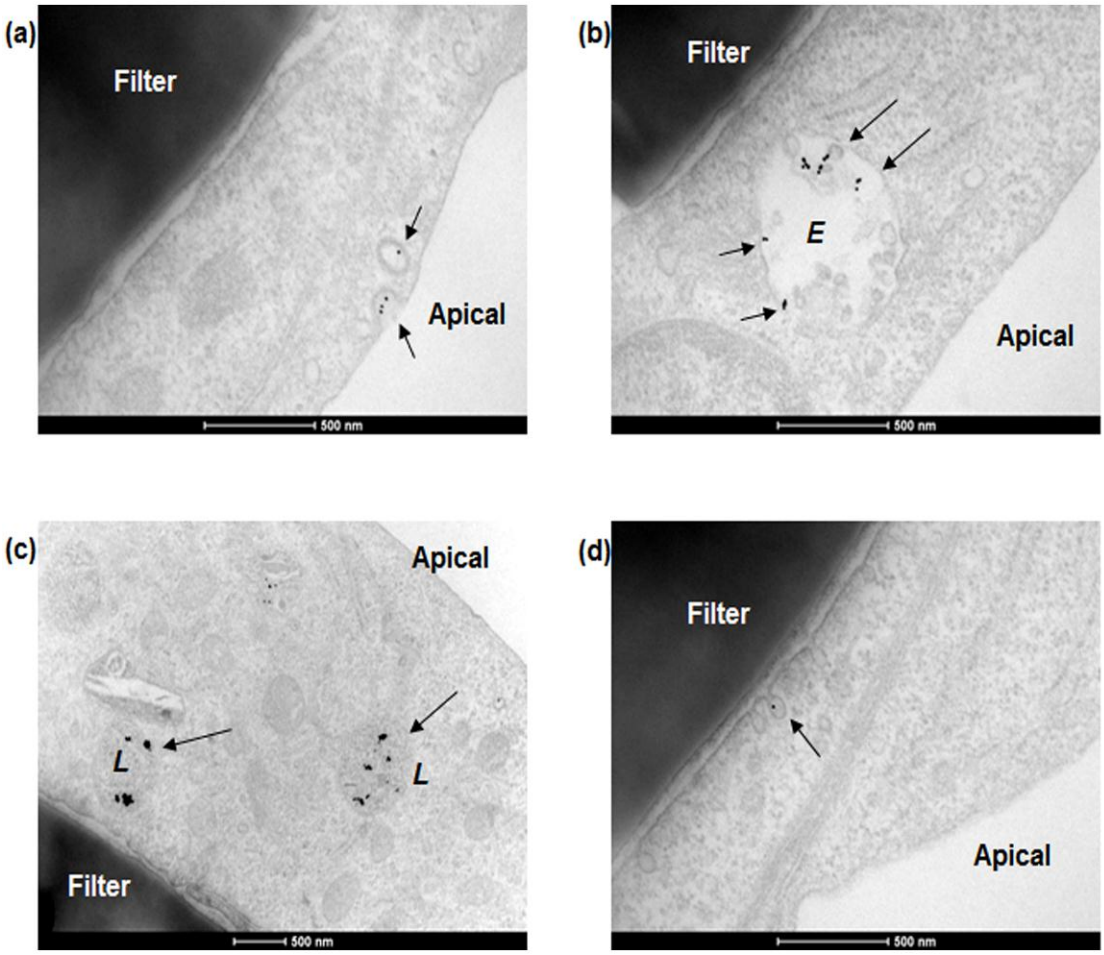

Figure S10. Uptake and transcytosis of 12 nm albumin-conjugated Au-NPs in hCMEC/D3 cell monolayers. Cells were exposed to 50 µg/ml nanoparticles in 2 % FBS assay medium for 4 hours. Nanoparticles were observed in (a) membrane invaginations closing on the apical cell membrane, and cytoplasmic vesicles; (b) early endosomes and (c) lysosomes. (d) A rare event suggestive of transcytosis was also observed for a single gold nanoparticle in a vesicle opening to the basal side of the cell.

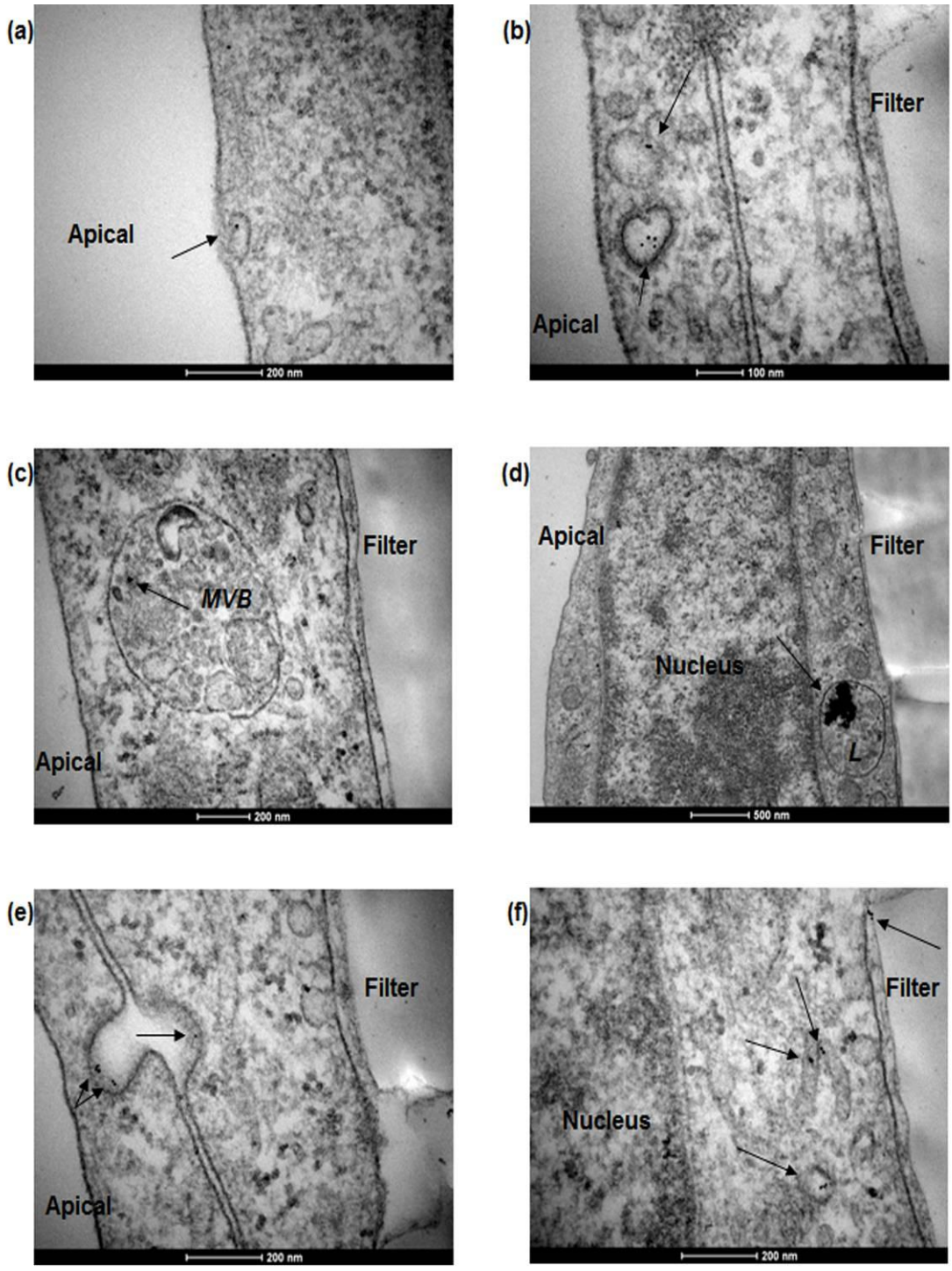

Figure S11. Uptake and transcytosis of 5 nm transferrin-conjugated Au-NPs in hCMEC/D3 cell monolayers. Cells were exposed to 50 µg/ml nanoparticles in 2 % FBS assay medium for 4 hours. (a) Single nanoparticles entering the cells into vesicles were observed, together with nanoparticles in other structures along the endo-lysosomal pathway, including (b) endocytic vesicles, (c) multivesicular bodies (*MVB*) and (d) lysosomes (*L*). (e) Au-NPs were also observed

in the intercellular space between two adjacent cells, close to membrane invaginations. (f) A few nanoparticles were also found outside the cells, close to the basal cell membrane (other nanoparticles inside the cells are also indicated by arrows).

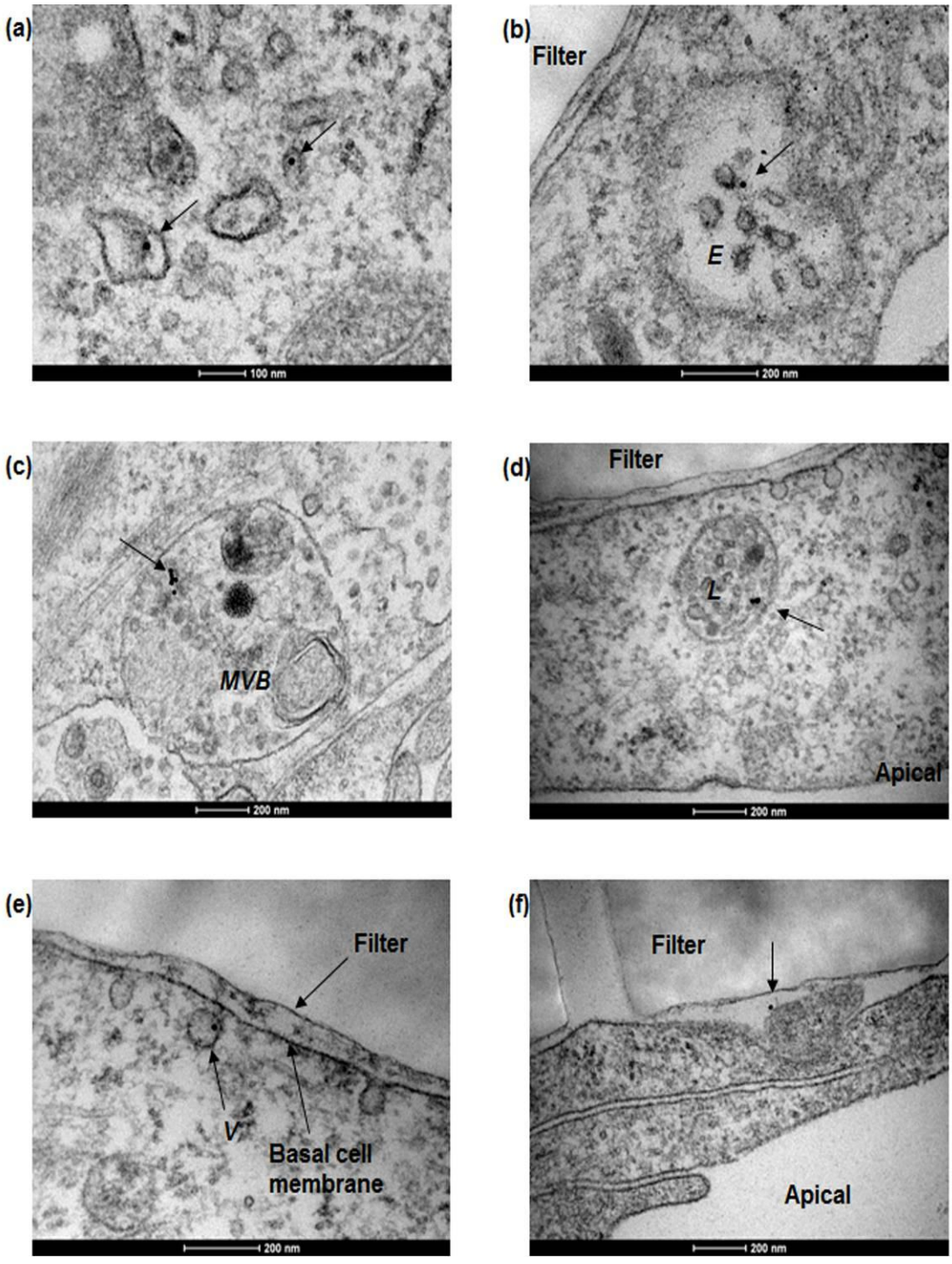

Figure S12. Uptake and transcytosis of 12 nm transferrin-conjugated Au-NPs in hCMEC/D3 cell monolayers. Cells were exposed to 50 µg/ml nanoparticles in 2 % FBS assay medium for 4 hours. Nanoparticles were observed in (a) endosomes, and (b) other endosomal structures (*E*), (c) multivesicular bodies (*MVB*) and (d) lysosomes (*L*). (e) A single Au-NP was also found in a

vesicle (*V*) approaching the basal membrane of the BBB layer, suggesting that particle export or transcytosis may occur. (f) A nanoparticle between the basal membrane and the filter surface, also suggestive of transcytosis.